ATLAS NOTE

ATLAS-CONF-2011-084

June 3, 2011

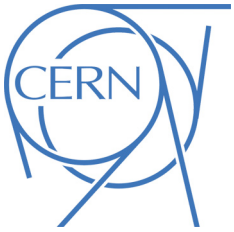

Measurement of the $W^{\pm}Z$ Production Cross-Section in Proton-Proton Collisions at $\sqrt{s} = 7$ TeV with the ATLAS Detector

The ATLAS Collaboration

Abstract

This note presents a measurement of $W^{\pm}Z$ production in 205 pb^{-1} of pp collision data at $\sqrt{s} = 7$ TeV collected by the ATLAS experiment in 2011. A total of 12 candidates with a background expectation of 2 events was observed for purely leptonically decaying bosons with electrons, muons and missing transverse energy in the final state. The total cross-section has been determined to be $\sigma^{\text{tot}}_{WZ} = 18^{+7}_{-6}$(stat) $\pm$3(syst) $\pm$1(lumi) pb in agreement with the Standard Model expectation.

1 Introduction

The underlying structure of the electroweak interactions in the Standard Model (SM) is the non-abelian $SU(2)_L \times U(1)_Y$ gauge group. This model has been very successful in describing current measurements. Features like vector boson masses and their coupling to fermions have been precisely tested at LEP and the Tevatron [1]. However, triple gauge boson couplings (TGC) predicted by this theory have not yet been determined with the same precision.

In the SM the TGC vertex is completely fixed by the electroweak gauge structure and so a precise measurement of this vertex, through the analysis of diboson production at the LHC, is essential to test the high energy behavior of electroweak interactions and to probe for possible new physics in the bosonic sector. Anomalous gauge boson couplings, a deviation from gauge constraints, might cause a significant enhancement of the production cross-section at high diboson invariant mass. Furthermore, new particles decaying into $W^{\pm}Z$ pairs are predicted in supersymmetric models with an extended Higgs sector (charged Higgs) as well as models with extra vector bosons (e.g. W') [2].

At the LHC, the dominant $W^{\pm}Z$ production mechanism is from quark-antiquark initial states and to a lesser extent from gluon-gluon fusion. Figure 1 shows the leading-order Feynman diagrams for $W^{\pm}Z$ production with $q\bar{q}'$ initial states.

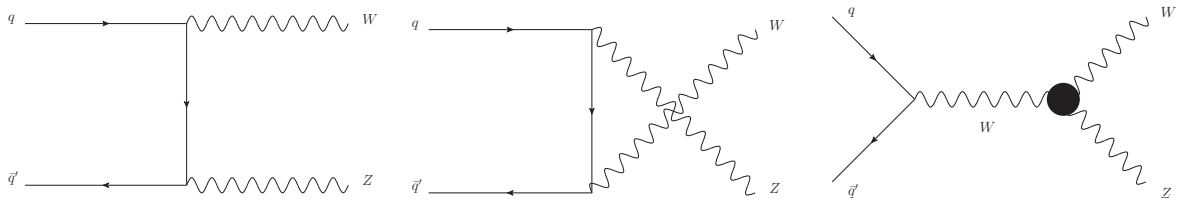

(a) t-channel (b) u-channel (c) s-channel

Figure 1: The SM tree-level Feynman diagrams for $W^{\pm}Z$ production through the (a) t-, (b) u- and (c) s-channel exchanges in $q\bar{q}$ interactions at hadron colliders. The s-channel diagram contains the WWZ TGC vertex.

This note presents a measurement of the $W^{\pm}Z$ production cross-section with the ATLAS detector in LHC proton-proton collisions at $\sqrt{s}$ = 7 TeV. The analysis uses four channels with leptonic decays ($W^{\pm}Z \to \ell\nu\ell\ell$) involving electrons and muons: eee, $ee\mu$, $\mu\mu e$ or $\mu\mu\mu$ (including secondary e or μ leptons from the decay of τ leptons) plus missing transverse energy, $E_{\mathrm{T}}^{\mathrm{miss}}$. The results are based on an integrated luminosity of 205 pb^{-1} collected by ATLAS in early 2011. The main sources of background to the leptonic $W^{\pm}Z$ signal are ZZ, $Z\gamma$, Z+jets, and top events. The signal and background contributions are mainly modeled with Monte Carlo simulation, validated with data-driven measurements.

Section 2 briefly describes the ATLAS detector and the data sample analyzed in this paper. Event triggering is discussed in Section 3. Section 4 discusses the signal and background simulation samples used in this analysis. The definition and reconstruction of physical observable objects such as particles and jets are detailed in Section 5, followed by event selection in Section 6. Section 7 presents the signal acceptance and background estimate, and the systematic uncertainties on these estimates. The results and cross-section calculation are given in Section 8.

2 The ATLAS Detector and Data Sample

The ATLAS detector is a multipurpose particle physics apparatus including a precision tracking system as the innermost part of the detector, highly segmented electromagnetic and hadronic calorimeters, and a large muon spectrometer [3].

This study uses data collected between March and May 2011. Data periods flagged with data quality problems that affect the reconstructed objects used in this analysis are removed. After data quality cuts, the total integrated luminosity used in this analysis is 205 pb^{-1}. The preliminary luminosity uncertainty for 2011 data is 4.5%. It is based on the 2010 luminosity calibration [4] which was transferred to the 2011 data by using the LAr forward calorimeter and the Tile calorimeter current measurements.

3 Online Sample Selection

The ATLAS trigger system consists of three stages: the hardware-based Level 1 (L1) trigger and the software-based Level 2 and Event Filter, which together are referred to as the High Level Trigger (HLT). For events with electromagnetic clusters, the transverse energy E_T is measured at L1 by trigger towers in a region of 0.1×0.1 in $\Delta\eta \times \Delta\phi$[1]. The L1 muon trigger utilizes a measurement of particle trajectories made by two parts of the muon detector: the Resistive Plate Chambers in the barrel region and the Thin Gap Chambers in the endcap region. Further requirements on the transverse momentum, p_T, are made by the HLT and additional quality criteria must be satisfied by electron candidates.

$W^{\pm}Z$ candidate events with multi-lepton final states are selected online with single muon and single electron triggers requiring p_T of at least 18 (20) GeV for muons (electrons). For events that pass all offline cuts, the $W^{\pm}Z$ trigger efficiencies for at least one single lepton trigger are 100.00±0.04%, 99.9±0.1%, 99.4±0.1%, and 98.7±0.1% for the final states eee, $ee\mu$, $e\mu\mu$, and $\mu\mu\mu$, respectively.

4 Simulated Data Samples

The $W^{\pm}Z$ production processes and subsequent pure leptonic decays are modeled by the MC@NLO [5] generator, with parton density function (PDF) set CTEQ6.6 [6], which incorporates the next-to-leading-order (NLO) QCD matrix elements into the parton shower by interfacing to the Herwig [7]/Jimmy [8] programs. The $W^{\pm}Z$ production cross-section from $q\bar{q}'$ annihilation is calculated to be $16.9^{+1.2}_{-0.8}$ pb [5]. Herwig is used to model the hadronization, initial state radiation and QCD final state radiation (FSR), photos [9] is used for QED FSR, Tauola [10] for the τ lepton decays, and Geant4 [11] for the simulated response of the ATLAS detector.

Major backgrounds for $W^{\pm}Z$ signal detection are jets associated with W or Z gauge bosons, and top-quark events. We use MC@NLO to model the $t\bar{t}$ and single top-quark events and Alpgen [12] and Pythia [13] to model the W/Z+jets and Drell-Yan backgrounds. Events with heavy flavor dijets are modeled with PythiaB [14]. The diboson processes WW, ZZ and $W/Z + \gamma$ are modeled with Herwig and MadGraph [15], respectively. Whenever leading order event generators are used, the cross-sections are corrected by using k-factors to NLO or NNLO (if available) matrix element calculations [5, 16, 17, 18, 19]. The simulated background event samples generally correspond to an integrated luminosity of 1–10 fb^{-1}.

All event samples are simulated with multiple interactions in bunch trains, including in-time and out-of-time pile-up, and with an average of 8 collision vertices per event. The number of interactions is re-weighted according to the luminosity distribution and the average number of interactions per bunch crossing of the data set used in this analysis, which varies according to the run period.

[1]Cylindrical coordinates (r, ϕ) are used in the transverse plane, ϕ being the azimuthal angle around the beam pipe. The pseudorapidity is defined in terms of the polar angle θ as $\eta = -\ln[\tan(\theta/2)]$.

5 Object Reconstruction

The main physical objects necessary to select $W^{\pm}Z$ events are electrons, muons, and $E_{\mathrm{T}}^{\mathrm{miss}}$. To ensure that the lepton candidates originate from the primary vertex, the longitudinal impact parameter with respect to the primary vertex must be less than 10 mm. Muons are identified by matching tracks reconstructed in the muon spectrometer to tracks reconstructed in the inner detector. Their momentum is calculated by combining information from the two track segments and correcting for the energy loss in the calorimeter. Only muons with $p_{\mathrm{T}} > 15$ GeV and $|\eta| < 2.4$ are considered. Non-prompt muons from hadronic jets are rejected by selecting only isolated muons, requiring the p_{T} sum of tracks within $\Delta R < 0.2$ of the muon[2] to be less than 10% of the muon p_{T}.

Electrons are formed by matching clusters found in the electromagnetic calorimeters to tracks in the inner detector. Electron candidates must have $E_T > 15$ GeV, where E_T is calculated from the cluster energy and track direction. To select central electrons and to avoid the transition regions between the calorimeters, the electron cluster must be within the regions $|\eta| < 1.37$ or $1.52 < |\eta| < 2.47$. Electrons are required to pass a stringent electron identification requirement based on shower shape, matched track quality, the ratio of the energy measured in the calorimeter to the momentum of the matched track, and the detection of transition radiation. To ensure isolation, the sum of the calorimeter energy in a cone of $\Delta R = 0.3$ around the electron candidate, not including the energy of the candidate itself, must be less than 6 GeV. This quantity is corrected for the additional energy deposited in the presence of pile-up, and a variable cut value chosen to maintain the same efficiency as a 6 GeV cut without the presence of pile-up. The electron energy in simulated events is smeared to account for a small difference between data and simulation. Electrons overlapping with selected muons within $\Delta R < 0.1$ are removed.

The $E_{\mathrm{T}}^{\mathrm{miss}}$ is calculated with calorimeter energy clusters in $|\eta| < 4.5$ and muons in $|\eta| < 2.7$. The clusters are calibrated as electromagnetic or hadronic energy according to cluster topology. A small correction avoids double-counting of the energy deposited by muons in the calorimeters.

6 Event Selection

At least one single electron or muon trigger is required to fire in order to select the event, as described in Section 3. At least one primary vertex, with at least 3 good tracks associated with it, is required to remove non-collision backgrounds and ensure good object reconstruction. Events with two leptons of the same flavour and opposite charge with an invariant mass within 10 GeV of the Z boson mass [20] are selected. This reduces much of the background from QCD and top production, and some diboson backgrounds as evident in the invariant mass distribution shown in Figure 2.

Events are then required to have at least 3 reconstructed leptons originating from the same primary vertex, two leptons from a $Z \to \ell\ell$ decay and an additional third lepton. This requirement reduces the Z+jets, top, and some diboson backgrounds, as can be seen in the distribution of the $E_{\mathrm{T}}^{\mathrm{miss}}$ in Figure 2. Next, the $E_{\mathrm{T}}^{\mathrm{miss}}$ in the event is required to be greater than 25 GeV and the transverse mass of the system formed from the third lepton and the $E_{\mathrm{T}}^{\mathrm{miss}}$ is required to be greater than 20 GeV. These cuts suppress the remaining backgrounds from Z and diboson production. For muon-(electron-) triggered events, at least one of the muons (electrons) is required to have $p_{\mathrm{T}} > 20$ (25) GeV to ensure that at least one triggered-object is well onto the efficiency plateau above the threshold of the primary single lepton trigger of 18 (20) GeV.

[2] ΔR is defined as $\Delta R = \sqrt{(\Delta\eta^2 + \Delta\phi^2)}$.

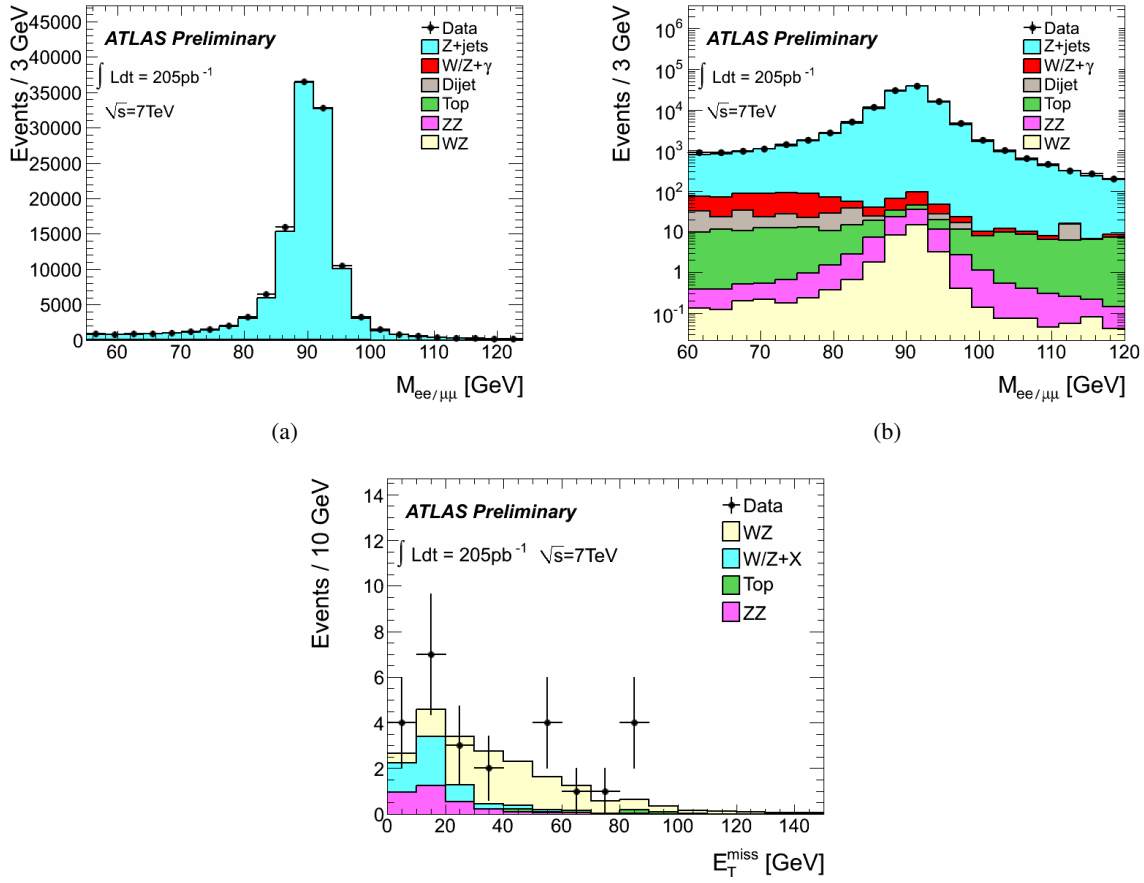

Figure 2: Invariant mass distribution of di-lepton pairs before the Z mass cut, in linear (a) and log (b) scale, and $E_{\mathrm{T}}^{\mathrm{miss}}$ distribution for the three-lepton events after the cut on the Z mass (c). The points represent observed event counts with error bars representing the Poisson standard deviation, whereas the stacked histograms are the MC predictions.

7 Signal Acceptance and Background Estimate

The acceptance of each cut is shown in Table 1 after all corrections have been applied for MC generated $W^{\pm}Z$ events decaying leptonically with electrons and muons in the final state.

Cutflow	Acceptance [%]
Muon or electron trigger	79.6 (79.6)
Primary Vertex	79.4 (99.8)
$\lvert m_{ll} - m_Z \rvert < 10$ GeV	28.3 (35.7)
Three leptons	11.8 (41.8)
$E_{\mathrm{T}}^{\mathrm{miss}} > 25$ GeV	9.4 (79.7)
$W^{\pm} M_T > 20$ GeV	8.8 (93.7)
Trigger Match	8.7 (98.7)

Table 1: Absolute (relative) acceptance after each cut was imposed on the MC sample of $W^{\pm}Z \to \ell\nu\ell\ell$ events, with ℓ being an electron or a muon, either from direct bosonic decay or from τ decay of the $W^{\pm}$ or Z.

The dominant backgrounds are events with jets associated with Z bosons, diboson production, and top-quark events. Backgrounds are estimated from simulation and data driven methods. For backgrounds which include at least one "fake" lepton (where fake lepton includes pion, kaon, and heavy quark decays to real leptons in addition to jets which fake lepton identification), two data-driven methods (fake factor method for fake electrons and matrix method for fake muons) with samples which have W/Z and jets in the final state are used.

In the fake factor method, the probability that a jet with a given p_{T} meeting loose quality and/or isolation requirements could pass the tight electron requirements (i.e. the fake factor) was measured in control samples of di-jet data. The full event selection was applied to the control sample, except for the $E_{\mathrm{T}}^{\mathrm{miss}}$ and W transverse mass criteria, for which selection efficiencies were estimated from MC and applied as normalization factors; the selection of at least three leptons was applied using the loose requirements. The resulting yields of events that had at least one object failing the tight requirements were then scaled by the relevant fake factors to get the background expectation.

In the matrix method, the muon isolation efficiency was measured in data for two samples: for non-prompt muons from heavy-flavour decays in jets in a sample of single muons with p_{T} between 15 and 20 GeV (extrapolated to higher p_{T} using simulated events), and for prompt muons using a tag and probe method on a sample of $Z \to \mu\mu$ decays. Samples of Z+muon events were then selected with and without the isolation requirement imposed on the non-Z muon. Using the number of events in these two samples, and the measured muon isolation efficiencies, the number of Z+non-prompt muon events in the isolated sample was estimated after subtracting the expected contribution from $t\bar{t}$ events. The resulting event yield was scaled by $E_{\mathrm{T}}^{\mathrm{miss}}$ and W transverse mass selection efficiencies estimated in MC to get the final background expectation.

The background from $W/Z + \gamma$ events, when the photon converts into an electron-positron pair, is not taken into account by the data-driven fake estimation methods, and is thus calculated with simulation. All other backgrounds are estimated using simulation.

For the electron and muon objects, the uncertainties associated with the reconstruction and identification efficiency, energy scale, energy smearing, and isolation are taken into account. The uncertainties are determined from comparisons between simulated events and data in control samples and are around 1%. For $E_{\mathrm{T}}^{\mathrm{miss}}$, uncertainties on the topological clusters and muon corrections to the $E_{\mathrm{T}}^{\mathrm{miss}}$ are considered, as well as uncertainties from the description of the pile-up conditions in data by the simulation. The dominant systematic contribution is from the description of the pile-up condition description for $E_{\mathrm{T}}^{\mathrm{miss}}$

and amounts to about 11%.

8 Results

The numbers of expected and observed events after applying all selection cuts are shown in Table 2. Statistical uncertainties are given for all four trilepton channels. We observe 12 $W^{\pm}Z$ candidates in data, with 9.1±0.2(stat)±1.3(sys) signal and 2.0±0.3(stat)±0.7(sys) background events expected. The signal definition includes the contribution from tau decays into electrons or muons, which accounts for about 0.5 events. The systematic uncertainty on the signal prediction is about 14%. Various kinematic variables and the $W^{\pm}$ charge of $W^{\pm}Z$ candidates are shown in Figure 3.

Final State	$eee + E_{\mathrm{T}}^{\mathrm{miss}}$	$ee\mu + E_{\mathrm{T}}^{\mathrm{miss}}$	$e\mu\mu + E_{\mathrm{T}}^{\mathrm{miss}}$	$\mu\mu\mu + E_{\mathrm{T}}^{\mathrm{miss}}$	combined
Observed	2	2	2	6	12
Signal	1.32±0.09	1.76±0.10	2.48±0.11	3.52±0.13	9.08±0.22±1.26
Bkg					
ZZ	0.028±0.003	0.12±0.01	0.08±0.01	0.18±0.01	0.40±0.01±0.05
W/Z+jets	0.09±0.02	0.17±0.04	0.24±0.07	0.52±0.08	1.02±0.12±0.50
Top	–	0±0.03	–	0.35±0.18	0.35±0.18±0.05
$W/Z+\gamma$	0.14±0.14	0 (< 0.05)	0.07±0.07	0 (< 0.05)	0.21±0.15±0.07
Bkg(tot)	0.25±0.14	0.29±0.05	0.39±0.10	1.05±0.19	1.98±0.27±0.67
S/B	5.3	6.2	6.3	3.3	4.6

Table 2: Summary of observed events and expected signal and background contributions in the four trilepton and combined channels. Statistical uncertainties are shown for the individual channels, and both statistical and systematic uncertainties are shown for the combined channel. Signal events ($W^{\pm}Z$) and background (ZZ, $W/Z+\gamma$) contributions are predicted from MC simulation. When no event passed the selection, the upper limit at 68% confidence level is quoted in brackets. Data driven background estimation methods are used for W/Z+jets for all decay channels, and top quarks in the eee and $e\mu\mu$ channels. The top background in the eee and $e\mu\mu$ channels is included together with the W/Z+jets background in the table.

8.1 Cross-Section Extraction

Cross-sections are obtained by maximizing likelihood functions (Equations 1 and 2).

$$L(\sigma^{\mathrm{fid}}_{WZ\to\ell\nu\ell\ell}) = \prod_{i=1}^{4} \frac{e^{-(N_s^i+N_b^i)} \times (N_s^i + N_b^i)^{N_{obs}^i}}{(N_{obs}^i)!}, \quad N_s^i = \sigma^i_{WZ\to\ell\nu\ell\ell} \times \mathcal{L} \times C^i \tag{1}$$

$$L(\sigma^{\mathrm{tot}}_{WZ}) = \prod_{i=1}^{4} \frac{e^{-(N_s^i+N_b^i)} \times (N_s^i + N_b^i)^{N_{obs}^i}}{(N_{obs}^i)!}, \quad N_s^i = \sigma^{\mathrm{tot}}_{WZ} \times B^i \times \mathcal{L} \times C^i \times A^i \tag{2}$$

In these expressions N_s^i is the number of expected signal events, N_b^i is the number of expected background events, and N_{obs}^i represents the number of observed events. B^i is the branching ratio, $\mathcal{L}$ is the integrated luminosity, C^i is the signal acceptance including a correction to remove the contribution from τ-decays in the fiducial phase space region defined below and A^i is the ratio of the number of events within the fiducial phase space region to the total number of generated events. The index i runs over each of the four decay channels $W^{\pm}Z \to e\nu ee$, $W^{\pm}Z \to \mu\nu ee$, $W^{\pm}Z \to e\nu\mu\mu$ and $W^{\pm}Z \to \mu\nu\mu\mu$, and $\ell = e, \mu$.

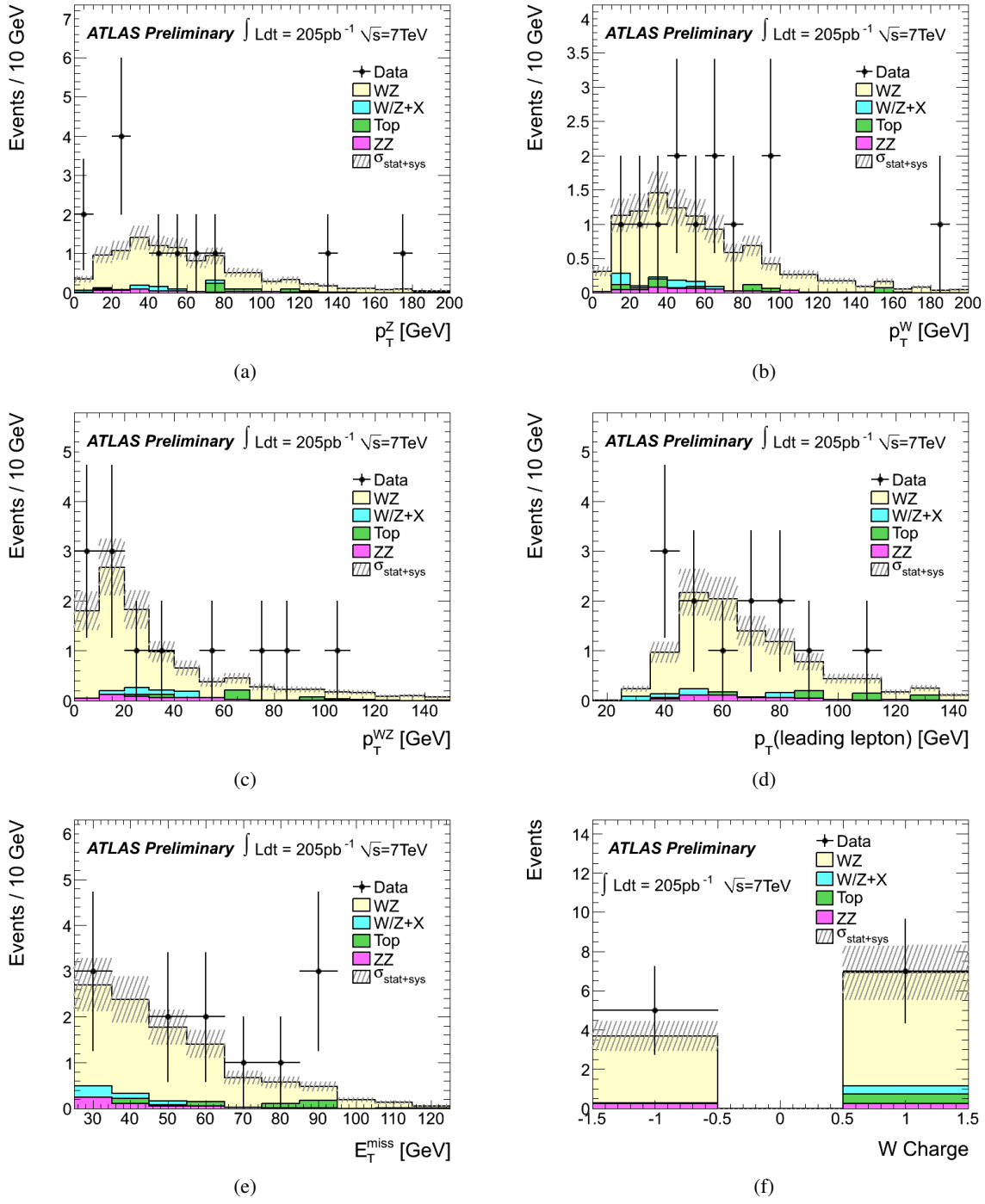

Figure 3: Distributions of various kinematic variables and the W charge of $W^{\pm}Z$ candidates. The kinematic variables shown include: (a) Transverse momentum of the Z (p_{T}^{Z}), (b) transverse momentum of the W (p_{T}^{W}), (c) transverse momentum of the $W^{\pm}Z$ system (p_{T}^{WZ}), (d) highest transverse momentum of any of the three leptons (p_{T}), (e) $E_{\mathrm{T}}^{\mathrm{miss}}$ and (f) $W^{\pm}$charge. The points represent observed event counts with error bars representing the Poisson standard deviation, whereas the stacked histograms are the predictions from simulation including the statistical and systematic uncertainty.

To combine the different channels a common phase space region is defined to extract a fiducial cross-section. The common phase space is defined as $p_{\mathrm{T}}^{\mu,e} > 15$ GeV, $|\eta^{\mu,e}| < 2.5$, $p_{\mathrm{T}}^{\nu} > 25$ GeV, $|M_{\ell\ell} - M_{\mathrm{Z\ Pole}}| < 10$ GeV, and $M_{\mathrm{T}}^{W} > 20$ GeV, and covers approximately the active detector volume.

In order to extrapolate to the total cross-section, the acceptance C^i in Equation 2 is scaled by the ratio A^i for each channel, calculated using the event generator information. This ratio A^i equals 0.37, 0.37, 0.35 and 0.34 for the $\mu\mu\mu$, $e\mu\mu$, $ee\mu$, and eee channels, respectively. The uncertainties on A^i due to the statistics of the signal MC are estimated to be about 2% (uncorrelated among channels) and included in the systematic uncertainties. The uncertainty due to the parton distribution functions, estimated to be about 0.8%, is not included in the experimental systematic uncertainties.

The final results for the combined fiducial cross section for the $W^{\pm}Z$ bosons decaying directly into electrons and muons excluding contributions from tau decays and the combined total inclusive cross-section measurements are shown below.

$$\sigma^{\mathrm{fid}}_{WZ\to\ell\nu\ell\ell} = 96^{+37}_{-30}(\mathrm{stat})\ ^{+15}_{-14}(\mathrm{syst})\ ^{+5}_{-5}(\mathrm{lumi})\ \mathrm{fb},\ \mathrm{with}\ \ell = e,\mu$$

$$\sigma^{\mathrm{tot}}_{WZ} = 18^{+7}_{-6}(\mathrm{stat})\ ^{+3}_{-3}(\mathrm{syst})\ ^{+1}_{-1}(\mathrm{lumi})\ \mathrm{pb}$$

The systematic uncertainties include all sources (assumed to be independent) except luminosity, which is listed separately. The systematic uncertainty is evaluated for each source for signal and background simultaneously. The resulting shifts in the cross-section are added in quadrature for all sources of systematic uncertainty.

9 Conclusion

A measurement of the $W^{\pm}Z$ production cross-section with the ATLAS detector in LHC proton-proton collisions at $\sqrt{s} = 7$ TeV has been performed using final states with electrons and muons. With an integrated luminosity of 205 pb^{-1} a total of twelve candidates is observed with a background expectation of 2.0±0.3(stat)±0.7(sys). The Standard Model expectation for the number of signal events is 9.1±0.2(stat)±1.3(sys). The fiducial and total cross-sections were determined to be respectively $\sigma^{fid}_{WZ\to\ell\nu\ell\ell} = 96^{+37}_{-30}(\mathrm{stat})\ ^{+15}_{-14}(\mathrm{syst})\ ^{+5}_{-5}(\mathrm{lumi})$ fb and $\sigma^{\mathrm{tot}}_{WZ} = 18^{+7}_{-6}(\mathrm{stat})\ ^{+3}_{-3}(\mathrm{syst})\ ^{+1}_{-1}(\mathrm{lumi})$ pb.

Good agreement with the Standard Model total cross-section [5] for this process of $16.9^{+1.2}_{-0.8}$ pb is observed. The result is shown in Figure 4 together with previous cross-section measurements of various gauge boson and $t\bar{t}$ production processes from ATLAS. All results are consistent with the SM expectations.

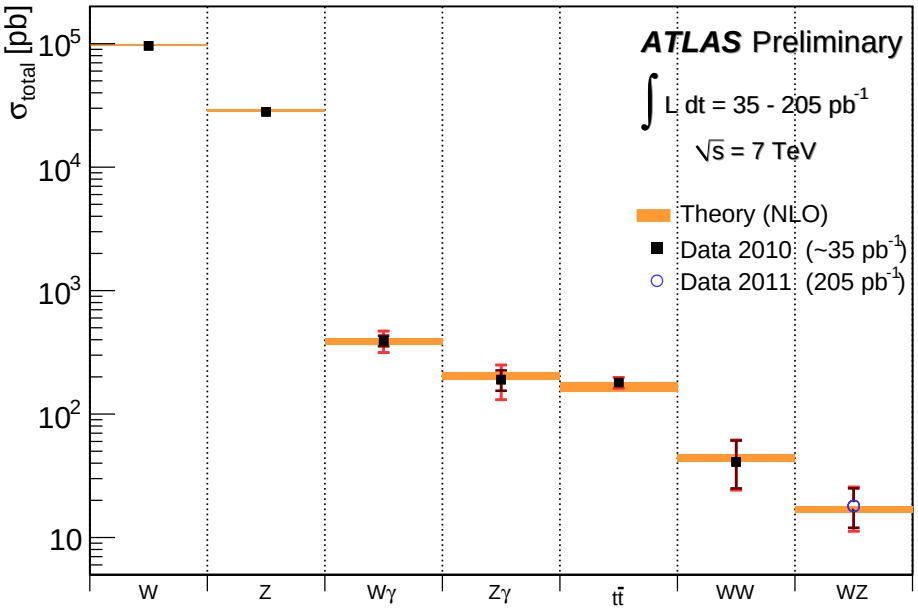

Figure 4: Summary of the $W^{\pm}Z$ production cross-section, reported in this note, together with previous ATLAS cross-section measurements from the 2010 dataset, including inclusive W and Z [21], diboson $W\gamma$ and $Z\gamma$ [22], WW [23] and $t\bar{t}$ [24] production. All measurements from the 2010 dataset were done with about 35 pb^{-1} of integrated luminosity. The dark error bar represents the statistical uncertainty. The red error bar represents the full uncertainty, including systematics and luminosity uncertainties.

References

[1] The ALEPH, CDF, D0, DELPHI, L3, OPAL, SLD Collaborations, the LEP Electroweak Working Group, the Tevatron Electroweak Working Group and the SLD electroweak and heavy flavour groups, *Precision Electroweak Measurements and Constraints on the Standard Model*, CERN-PH-EP-2010-095 (2010) , arXiv:hep-ex/1012.2367.

[2] L. Dixon, Z. Kunzst, and A. Signer, *Vector Boson Production in Hadron Collisions at order α_s: Lepton Correlations and Anomalous Couplings*, Phys. Rev D **60** (1999) 114037, arXiv:hep-ph/9907305v1.

[3] ATLAS Collaboration, *The ATLAS experiment at the CERN Large Hadron Collider*, JINST **3** **S08003** (2008) .

[4] ATLAS Collaboration, *Updated Luminosity Determination in pp Collisions at $\sqrt{s}$ =7 TeV using the ATLAS Detector*, ATLAS-CONF-2011-011 (Mar, 2011) .

[5] S. Frixione and B. R. Webber, *Matching NLO QCD computations and parton shower simulations*, JHEP **06** (2002) 029, hep-ph/0204244.

[6] P. M. Nadolsky et al., *Implications of CTEQ global analysis for collider observables*, Phys. Rev. **D78** (2008) 013004, arXiv:hep-ph/0802.0007.

[7] G. Corcella et al., *HERWIG 6: an event generator for Hadron Emission Reactions With Interfering Gluons (including supersymmetric processes)*, JHEP **01** (2001) 010, arXiv:hep-ph/0011363.

[8] J. M. Butterworth, J. R. Forshaw, and M. H. Seymour, *Multiparton interactions in photoproduction at HERA*, Z. Phys. **C72** (1996) 637, arXiv:hep-ph/9601371.

[9] P. Golonka and Z. Was, *PHOTOS Monte Carlo: A Precision tool for QED correction in Z and W decays*, Eur. Phys. J. C **45** (2006) 97.

[10] R. Decker, S. Jadach, J. Kuhn, and Z. Was, *The tau decay library TAUOLA, Version 2.4*, Comput. Phys. Commun. **76** (1993) 361.

[11] S. Agostinelli et al., *GEANT4: A Simulation toolkit*, Nucl. Instrum. Meth. **A506** (2003) 250.

[12] M. L. Mangano, M. Moretti, F. Piccinini, R. Pittau, and A. Polosa, *ALPGEN, a generator for hard multiparton processes in hadronic collisions*, JHEP **07** (2003) 001, arXiv:hep-ph/0206293.

[13] T. Sjostrand et al., *High-energy physics event generation with PYTHIA 6.1*, Comput. Phys. Commun. **135** (2001) 238, arXiv:hep-ph/0010017.

[14] S. P. Baranov and M. Smizanska, *Semihard b quark production at high-energies versus data and other approaches*, Phys. Rev. **D62** (2000) 014012.

[15] J. Alwall et al., *MadGraph/MadEvent v4: The New Web Generation*, JHEP **09** (2007) 028, arXiv:hep-ph/0706.2334.

[16] J. M. Campbell and R. K. Ellis, *An update on vector boson pair production at hadron colliders*, Phys. Rev. **D60** (1999) 113006, arXiv:hep-ph/9905386.

[17] C. Anastasiou, L. J. Dixon, K. Melnikov, and F. Petriello, *High precision QCD at hadron colliders: Electroweak gauge boson rapidity distributions at NNLO*, Phys. Rev. **D69** (2004) 094008, arXiv:hep-ph/0312266.

[18] R. Hamberg, W. L. van Neerven, and T. Matsuura, *Erratum to: "A complete calculation of the order α_s^2 correction to the Drell-Yan K-factor"[Nucl. Phys. B 359 (1991) 343]*, Nucl. Phys. **B 644** (2002) 403–404.

[19] T. Binoth, M. Ciccolini, N. Kauer, and M. Kramer, *Gluon-induced W-boson pair production at the LHC*, JHEP **12** (2006) 046, arXiv:hep-ph/0611170.

[20] K. Nakamura et al. (Particle Data Group), *Review of Particle Physics*, J. Phys. G **37** (2010) 075021.

[21] ATLAS Collaboration, *A measurement of the total $W^{\pm}$ and Z/γ^* cross sections in the e and μ decay channels and of their ratios in pp collisions at $\sqrt{s} = 7$ TeV with the ATLAS detector*, ATLAS-CONF-2011-041 (Mar, 2011) .

[22] ATLAS Collaboration, *Measurement of the production cross section of $W\gamma$ and $Z\gamma$ at $\sqrt{s} = 7$ TeV with the ATLAS Detector*, to be submitted to Phys. Lett. B (2011) .

[23] ATLAS Collaboration, *Measurement of the WW cross section in sqrt(s) = 7 TeV pp collisions with ATLAS*, submitted to Phys. Rev. Lett. (Apr, 2011) , arXiv:hep-ex/1104.5225.

[24] ATLAS Collaboration, *A combined measurement of the top quark pair production cross-section using dilepton and single-lepton final states*, ATLAS-CONF-2011-040 (Mar, 2011) .